

Effect of sodium hexametaphosphate on the flotation separation of lepidolite and quartz: MD study

Siqi Yang ^{1,2,3}, Xianping Luo ^{1,2,3,5}, Hepeng Zhou ^{1,2,3,5}, Xuekun Tang ^{1,2,3,5}, Zishuai Liu ^{1,2,3,5}, Jiangfeng Guo ^{1,2,3}, Louyan Shen ⁴

¹ Jiangxi Province Key Laboratory of Efficient Development and Utilization of Rare Metal Resources, Jiangxi University of Science and Technology, Ganzhou 341000, China

² Jiangxi Provincial Key Laboratory of Low-Carbon Processing and Utilization of Strategic Metal Mineral Resources, Jiangxi University of Science and Technology, Ganzhou 341000, China

³ Faculty of Resource and Environmental Engineering, Jiangxi University of Science and Technology, Ganzhou 341000, China

⁴ China Nerin Engineering Co., Ltd., China

⁵ Yichun Lithium New Energy Industry Research Institute, Jiangxi University of Science and Technology, Yichun 336000, China

Corresponding authors: luoxianping9491@163.com (X. Luo), txk0797@126.com (X. Tang)

Abstract: The present study employed sodium hexametaphosphate (SHMP) as a depressant for quartz to achieve selective flotation separation of lepidolite. Micro-flotation and artificial mixed-mineral tests confirmed that the introduction of SHMP successfully facilitated the separation of lepidolite and quartz under weak acid conditions. The MD simulations revealed that hydroxylation of non-bridging oxygen atoms on the quartz surface influenced the adsorption of dodecylamine (DDA), while it had no impact on the adsorption of sodium hexametaphosphate (SHMP). Additionally, SHMP was found to form hydrogen bonds with hydroxyl groups present on the quartz surface, thereby enhancing its adsorption capacity and indirectly promoting a higher degree of surface hydroxylation to impede DDA adsorption, thus preserving the hydrophilic nature of the quartz surface. Conversely, the dissolution of K^+ in the $[Si_{6-n}Al_nO_6]$ ($n=0, 1, 2$) rings on the lepidolite surface in an aqueous environment leads to a negative charge on lepidolite. This negatively charged state presents obstacles for SHMP adsorption onto the lepidolite surface; however, it facilitates strong attraction and firm adsorption of positively charged DDA within the ring cavities of lepidolite, resembling an "anchor". The adsorption test revealed that, following treatment with SHMP, a substantial amount of DDA remained adsorbed onto the lepidolite, while only a negligible quantity was observed on the quartz surface. Consequently, the introduction of SHMP enables effective inhibition of quartz under conditions characterized by low hydroxylation levels on its surface (weak acid or neutral), thereby facilitating the production of high-quality lepidolite products.

Keywords: lepidolite, quartz, hydroxylation, Molecular Dynamics, adsorption difference

1. Introduction

Lithium is a critical component in the production of lithium-ion batteries, which serve as the primary means of energy storage in the emerging new energy industry (Xiao et al., 2023). To mitigate global greenhouse gas emissions and expedite the achievement of "carbon neutrality and peak carbon" strategic goals, there is an active global promotion of the lithium-based new energy industry (Guo et al., 2021). Consequently, there has been a steady increase in demand for lithium resources. In order to ensure a consistent market supply of lithium raw materials, extracting lithium from lepidolite has become an indispensable method of resource extraction (Liu., 2023; Zhang et al., 2023). Lepidolite naturally occurs closely associated with other silicate minerals in deposits, with quartz being a common

example (Choi et al., 2012; Wang et al., 2014). Currently, a significant portion of lepidolite products are obtained from such deposits.

Froth flotation is a widely employed and cost-effective process for extracting lepidolite products from granite deposits due to its high separation efficiency (Korbel et al., 2021; Tadesse et al., 2019). Research efforts have primarily focused on the development of innovative collectors, such as Gemini amine-based collectors and amidoxime collectors, for lepidolite flotation (Huang et al., 2022; Huang et al., 2022). Although these collectors have demonstrated promising performance in laboratory tests, further validation in industrial settings is imperative to ascertain their suitability for large-scale production. In the field of flotation industry, cationic amine collectors like dodecylamine and octadecylamine are commonly utilized to enhance the floatability of lepidolite (Liu et al., 2015; Liu et al., 2022). The adherence of these collectors to the lepidolite surface results in the formation of hydrophobic layers, thereby enhancing the floatability of lepidolite. However, separating lepidolite from quartz has long posed a significant challenge due to their comparable adsorption capacity for collectors (Wei et al., 2021). Consequently, the effectiveness of lepidolite separation from quartz is considered a crucial indicator for evaluating the efficiency and success of the overall flotation process in lepidolite recovery (Vieceli et al., 2016). This parameter holds substantial significance in assessing the efficacy of the lepidolite recovery process.

In order to enhance the separation of lepidolite from quartz during flotation processes, the addition of depressants is essential. Sodium silicate and starch are two commonly utilized depressants (Ai et al., 2014; Peng et al., 2016). However, it has been demonstrated that the use of sodium silicate as a depressant lead to indiscriminate flotation of silicate minerals and vein minerals (Irannajad et al., 2009). Moreover, one major drawback associated with the utilization of sodium silicate is its substantial dosage requirement (Wang et al., 2016; Meng et al., 2019), which inevitably poses significant challenges in treating wastewater with high COD and very slow settling rates due to a large number of siliceous colloids (Tian et al., 2018). Another study indicated that muscovite can be obtained by employing calcium lignosulphonate as a depressant for quartz and feldspar, along with conventional amines as muscovite collectors (Korbel et al., 2023). Flotation tests conducted on pure minerals and actual ore samples revealed that the concentration of the agent significantly influences flotation. Generally, compared to lepidolite collectors, progress in developing depressants for effective flotation separation between lepidolite and other silicate ore veins has been relatively sluggish. Consequently, further research is warranted in this field.

Sodium hexametaphosphate (SHMP), with the chemical formula $(\text{NaPO}_3)_6$, is highly soluble in water and possesses strong metal complexing properties. As a result, it finds extensive application as an inorganic depressant in mineral processing operations (Yang et al., 2023; Zhang et al., 2021). Numerous studies have demonstrated its significant depressant effect on specific minerals. For instance, during flotation of molybdenum oxide and fluorapatite systems, SHMP exhibits a more pronounced suppressive impact on fluorapatite compared to molybdenum oxide (Liu et al., 2021). These findings clearly indicate the excellent selectivity of SHMP in the flotation process involving pure minerals of molybdenum oxide and fluorapatite. In a study investigating scheelite and calcite flotation, selective chemisorption of Ca^{2+} by SHMP was observed specifically on calcite due to its higher calcium activity and density relative to scheelite surfaces (Guan et al., 2024). Furthermore, research into the dispersion properties of serpentine revealed that sodium hexametaphosphate can modify the zeta potential of serpentine while selectively dispersing valuable minerals such as nickel pyrite (Lu et al., 2019). In recent years, several studies have explored the effectiveness of SHMP as a dispersant/depressant with positive outcomes (Liao et al., 2022; Wang et al., 2022).

However, despite the existence of these studies, there is limited information available regarding the action of sodium hexametaphosphate (SHMP) in silicate flotation systems. For instance, the underlying mechanism behind the depressant effect of SHMP in lepidolite and quartz flotation systems has not been systematically elucidated. Therefore, this study aims to investigate the flotation behavior of lepidolite and quartz through micro-flotation tests utilizing single minerals as well as artificially mixed minerals with SHMP acting as a depressant and dodecylamine (DDA) serving as a collector. Additionally, molecular dynamics simulation and adsorption measurement will be employed to analyze the adsorption phenomenon and mechanism of SHMP on the surface of these two minerals.

2. Experimental

2.1. Materials and reagents

The lepidolite and quartz utilized in this experiment were sourced from Peshawar, Pakistan and Yichun, China, respectively. The lepidolite was obtained as purple-red lamellae, while the quartz was acquired as white (translucent) lumps. Both minerals were pulverized using an agate mortar and subsequently sieved into three size fractions (+74 μm , -74+38 μm , and -38 μm) utilizing a top-impact vibrating sieve. The +74 μm fraction was reground to achieve a particle size of -74+38 μm . The resulting -75+38 μm samples underwent ultrasonic washing with deionized water for 5 minutes each, followed by drying in a vacuum oven at 40°C to obtain the final products of lepidolite and quartz. To confirm the purity of these minerals, XRD analysis and chemical composition analyses were conducted on both samples. The results demonstrated that the purity of both minerals exceeded 95% and met the requirements of the test. These analytical findings are presented in Fig. 1 and Table 1.

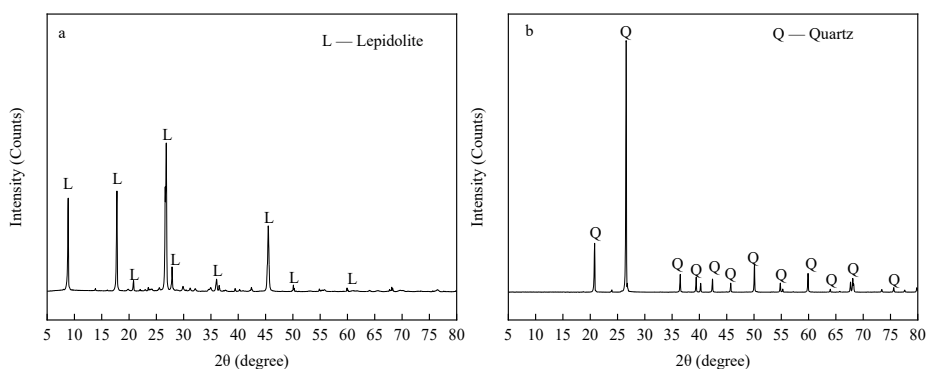


Fig. 1. X-ray diffraction patterns of (a) lepidolite and (b) quartz

Table 1. Results of mineral chemical fraction analysis (%)

| component | Li ₂ O | SiO ₂ | Al ₂ O ₃ | Fe ₂ O ₃ | K ₂ O | Other |
|------------|-------------------|------------------|--------------------------------|--------------------------------|------------------|-------|
| lepidolite | 5.47 | 53.5 | 27.16 | 0.82 | 10.02 | 3.03 |
| quartz | — | 98.47 | 1.06 | 0.19 | 0.12 | 0.16 |

Sodium hexametaphosphate (SHMP, purity: 99%) purchased from Shanghai Macklin Biochemical Co., Ltd. was used as depressant. Dodecylamine (DDA, purity: 99%), HCl and NaOH (purity: 99%) purchased from Xilong Scientific Co., Ltd. were as collector and regulators. Deionized water was used in the entire test and measurements.

2.2. Micro-flotation tests

The pure mineral micro-flotation tests were conducted using a suspended flotation machine (XFGII5, Jilin Exploration Machinery Factory) equipped with a flotation cell (volume: 40 ml) and an impeller speed set at a constant 1900 rpm throughout the flotation process. For single mineral micro-flotation, a homogeneous slurry was formed by adding 2 g of mineral sample and 35 ml of deionized water to the cell. The pH of the slurry was adjusted to the desired value using HCl and NaOH solutions (0.1 mol/L). After stirring for 3 minutes, specified doses of depressant (SHMP) and collector (DDA) were successively added at intervals of 3 minutes each. Following an additional minute of stirring, aerated flotation was performed, and the resulting floating froth product was manually collected for 3 minutes. The froth product and tailings were then filtered, dried, and weighed to calculate recovery based on their weight distribution. In the case of mixed binary minerals micro-flotation test involving lepidolite and quartz in a mass ratio of 1:1, the same flotation process as that used for single mineral flotation test was followed. At the end of this process, chemical determination of Li₂O content in the froth product was carried out to calculate its recovery based on both froth product's Li₂O grade as well as raw ore's Li₂O grade. All micro-flotation tests were repeated three times and the mean was taken as the final value. Error bars represent one standard deviation from the mean.

2.3. Molecular dynamics simulation

2.3.1. Mineral and agent models

The lepidolite and quartz crystal structures were taken from the American Mineralogist Crystal Structure Database and used as the initial input structures for the MD experiments (Liu et al., 2015). Lepidolite is a prototypical layered silicate mineral composed of two layers of $[\text{SiO}_4]$ tetrahedral sheets and one layer of $[\text{AlO}_6]$ octahedral sheets, with lithium typically occupying the octahedral position. Within the $[\text{SiO}_4]$ tetrahedral structure, approximately one-eighth of the silicon atoms are substituted by aluminum atoms, while potassium ions are employed in the interlayer to balance the charge loss resulting from this substitution. The unit cell parameters of the monoclinic $C2/c$ $2M_2$ lepidolite are: $\alpha = 90^\circ$, $\beta = 99.48^\circ$, $\gamma = 90^\circ$, $a = 9.023 \text{ \AA}$, $b = 5.197 \text{ \AA}$, $c = 20.171 \text{ \AA}$. Based on chemical analysis, we provide a structural formula applicable to lepidolite simulation: $\text{K}\{\text{Li}_{2-x}\text{Al}_{(1+x)}[\text{Al}_{2x}\text{Si}_{(4-2x)}\text{O}_{10}](\text{O},\text{F})_2\}$ ($x=0-0.5$). To facilitate the establishment of the adsorption substrate, the quartz unit cell was orthogonalized resulting in $\alpha = \beta = \gamma = 90^\circ$, $a = 4.913 \text{ \AA}$, $b = 8.510 \text{ \AA}$, $c = 5.4052 \text{ \AA}$. The two mineral structures are illustrated in Fig. 2.

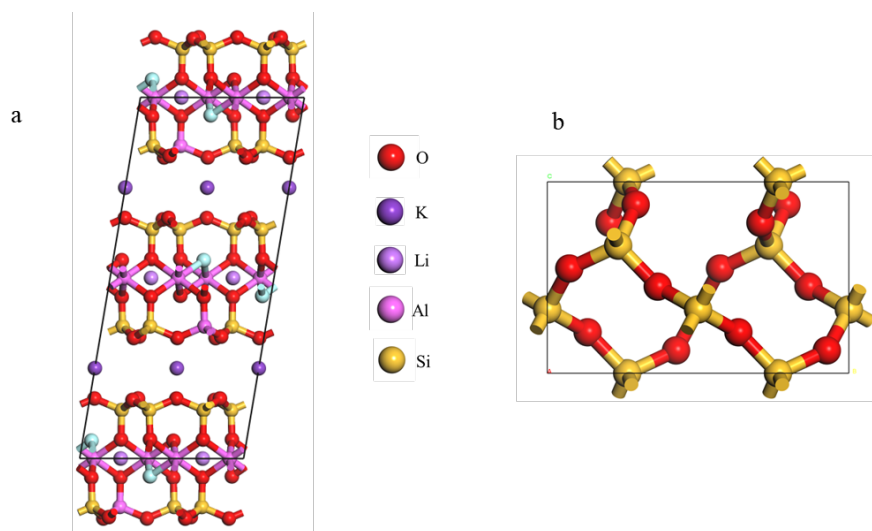


Fig. 2. The mineral structures of (a) lepidolite and (b) quartz

The structures of the two agents were optimized using the DMol3 module of Materials Studio 8.0 software, employing the GGA/PBE method within density functional theory. For simulating water molecules, an extended version of the simple point charge model (SPC/E) was utilized. The molecular structures of the two agents are illustrated in Fig. 3.

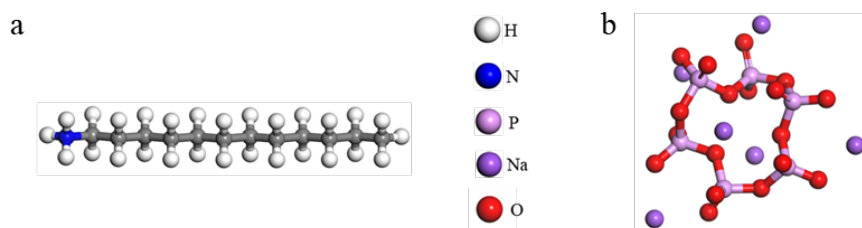


Fig. 3. The molecular structures of (a) DDA and (b) SHMP

2.3.2. Solid/liquid interface model

Firstly, the (001) crystal plane was selected as the primary dissociation surface for lepidolite due to its predominant dissociation behavior. Similarly, for quartz crystals, the (001) crystal plane was predicted to be relatively stable (Liu et al., 2019). To create reconstructed reactive solid-phase substrates, supercells of $5 \times 3 \times 1$ and $5 \times 3 \times 3$ were employed for lepidolite and quartz, respectively. In the natural environment, hydroxylation of the quartz (001) surface occurs due to the susceptibility of non-bridging oxygen bonds formed during quartz fragmentation to undergo hydroxylation in an aqueous

environment (Zhang et al., 2023). Moreover, this study did not account for the dissolution of potassium ions on the lepidolite (001) surface as they would be solubilized in water during the actual flotation process. Secondly, the liquid phase system was established using the Amorphous Cell module in MS 8.0, following the guidelines provided in Tables 2 and 3. This system comprised water molecules, pharmaceuticals, as well as Na⁺ and Cl⁻ ions. The concentration of water molecules has been established at 1g/cm³. The inclusion of Na⁺ and Cl⁻ ions aimed to ensure charge balance within the reaction system. In order to study the adsorption process of the agent on the mineral surface, the agent molecules were placed closer to the mineral surface. Finally, a solid/liquid (S/L) reaction system was constructed using the Build Layer tool with a 120 Å vacuum layer introduced to prevent periodic interactions between upper and lower mineral surfaces as illustrated in Fig. 4.

Table 2. The number of water molecules, inorganic ions and agents in lepidolite systems

| Systems | DDA | SHMP | Na ⁺ | Cl ⁻ | H ₂ O |
|---------|-----|------|-----------------|-----------------|------------------|
| A1 | 5 | - | 15 | 5 | 1000 |
| A2 | 10 | - | 15 | 10 | 1000 |
| A3 | 15 | - | 15 | 15 | 1000 |
| B1 | - | 5 | 20 | 5 | 1000 |
| B2 | - | 10 | 20 | 5 | 1000 |
| B3 | - | 15 | 20 | 5 | 1000 |
| AB | 15 | 10 | 15 | 15 | 1500 |

Table 3. The number of water molecules, inorganic ions and agents in quartz systems

| Systems | DDA | SHMP | Na ⁺ | Cl ⁻ | H ₂ O |
|---------|-----|------|-----------------|-----------------|------------------|
| C1 | 5 | - | 15 | 20 | 1000 |
| C2 | 10 | - | 10 | 20 | 1000 |
| C3 | 15 | - | 5 | 20 | 1000 |
| D1 | - | 5 | 10 | 10 | 1000 |
| D2 | - | 10 | 10 | 10 | 1000 |
| D3 | - | 15 | 10 | 10 | 1000 |
| CD | 15 | 10 | 15 | 15 | 1500 |

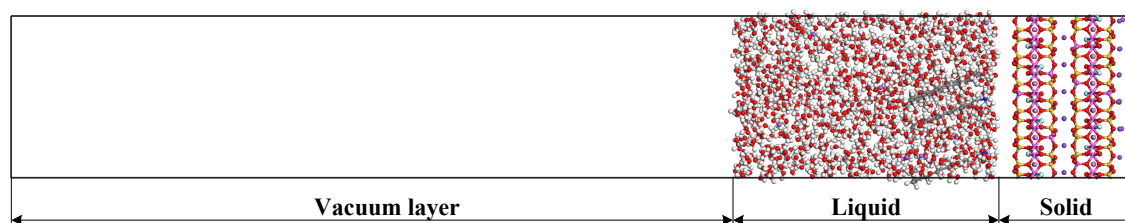


Fig. 4 The diagram illustrates a solid/liquid phase (S/L) reaction system

2.3.3. Simulation methods

All simulations were performed using Accelrys software (Materials Studio 8.0). In this work we used PCFF-interface as a force field as it has been shown to be suitable for calculations of silicate minerals (Heinz et al., 2013; Bai et al., 2023). An energy-minimizing optimization of these models is first performed once through in the PCFF-interface force field, ensuring that the initial model has the lowest energy and reduces abnormal intermolecular contacts (especially between the agent molecules and the mineral surface). Immediately after ensuring that all atoms were free to move, the MD simulations were carried out for 2 ns using an NHL thermostat set to a temperature of 298 K and a simulation step size of 1.0 fs under a canonical systematic system (NVT). The structures after these optimizations mentioned above were used as initial configurations for the final MD simulations. The final molecular dynamics

simulations were carried out for all systems for 0.5 ns, and the equilibrium dynamic trajectories of each model were recorded at 10 fs intervals for statistical analyses, the electrostatic forces were solved using the Ewald method, and the van der Waals forces were solved using the Atom based method, and the truncation energy was set to be 12.5 Å. The interactions of the agent molecules with the lepidolite (001) and the quartz (001) energy were calculated according to equation (1):

$$\Delta E = \frac{E_{\text{complex}} - E_{\text{reagent}} - E_{\text{minerals}}}{N} \quad (1)$$

The variables E_{complex} , E_{reagent} and E_{minerals} represent the energy of the agent-mineral system, mineral molecules, and agent molecules respectively. N denotes the number of agents. When the adsorption energy $\Delta E > 0$, it indicates a low affinity of the molecules for surface adsorption. A higher value of ΔE corresponds to a more challenging adsorption process. Conversely, when $\Delta E < 0$, it signifies a decrease in total system energy upon molecule-surface adsorption. A more negative ΔE implies a stronger interaction between agent molecules and mineral surfaces.

2.4. Adsorption measurement

Adsorption quantification employed the residual concentration method utilizing a Multi N/C 3100 Total Organic Carbon analyzer (Jena Analytical Instruments GmbH, Germany). A pristine beaker containing 2g of mineral served as the vessel while reagents were incrementally introduced to attain target concentrations. Following agitation, separation of mixtures occurred via high-speed centrifugation. Subsequently, measurement of TOC concentration in supernatants facilitated calculation of collector's remaining concentration employing equation (2), thereby determining its adsorption capacity across various conditions. Fig. 5 depicts an illustrative adsorption curve for a standardized dodecylamine solution.

$$\Gamma = \frac{(C_0 - C_x) \times V}{m} \quad (2)$$

where Γ is the adsorbed volume. C_0 is the initial concentration of dodecylamine in the pulp, and C_x is the residual concentration of dodecylamine in the supernatant after interaction with the mineral and after centrifugation. V is the volume of the solution, and m is the mass of the mineral, 2 g.

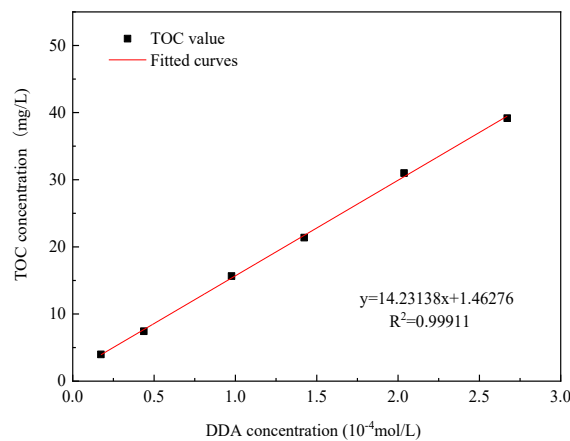


Fig. 5. The adsorption curve for the standard concentration of DDA solution

3. Results and discussion

3.1. Micro-flotation results

Micro-flotation tests were carried out to evaluate the effect of SHMP on flotation behavior of lepidolite and quartz.

The recovery of lepidolite consistently outperformed that of quartz in the absence of SHMP, as illustrated in Fig. 6, indicating the superior collection efficiency of DDA for lepidolite. Furthermore, the recovery of lepidolite decreased with increasing pH, while the recovery of quartz exhibited an upward trend and surpassed a declining point beyond pH 7.0. At pH 3, the recovery rate for lepidolite could exceed 90%, whereas only 21.34% recovery was achieved for quartz, demonstrating the feasibility of

separating lepidolite and quartz under highly acidic conditions. Upon addition of SHMP within the pH range from 3.0 to 6.0, the recovery rate for quartz dropped below 5%, while that for lepidolite experienced only a slight decrease (still above 80%), thereby amplifying the disparity in floatability between these two minerals and highlighting SHMP's inhibitory effect on quartz floatability. As pH further increased, there was a marginal increase in quartz recovery but a continued decline in lepidolite recovery; ultimately reaching maximum disparity between them at pH 5.0.

The results presented in Fig. 7 demonstrate a significant decrease in quartz recovery with increasing SHMP dosage, while the recovery of lepidolite exhibits only a slight decline but remains at a high level. Furthermore, as the concentration of SHMP increases, this discrepancy in recovery becomes more pronounced. In other words, the addition of SHMP impedes the flotation recovery of quartz by DDA due to its inhibitory effect on the quartz surface. However, DDA still displays considerable adsorption on the surface of lepidolite, enabling it to be entrained into the froth layer. At an SHMP dosage of 0.8×10^{-4} mol/L, complete suppression of quartz is achieved while lepidolite maintains over 85% recovery.

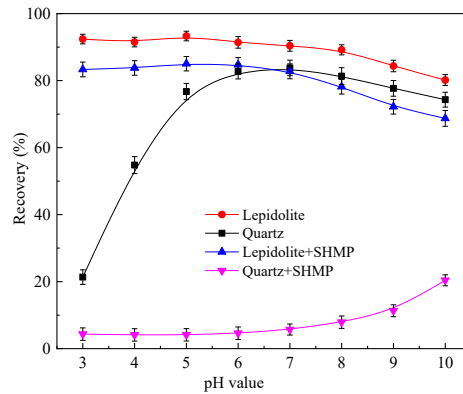


Fig. 6. Effect of SHMP on flotation recovery of lepidolite and quartz under different pH conditions

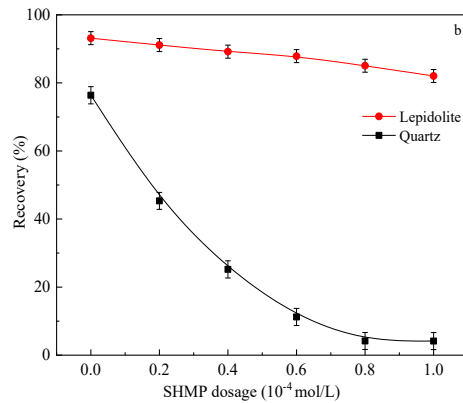


Fig. 7. Effect of SHMP dosage on flotation recovery of lepidolite and quartz

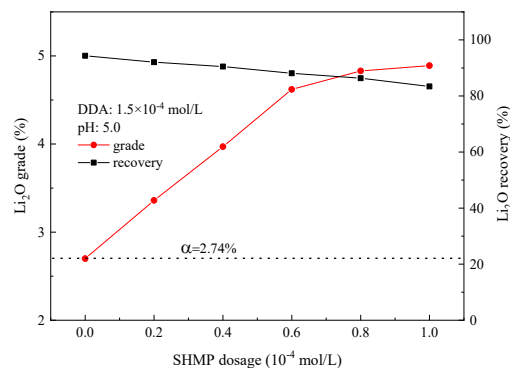


Fig. 8. Relationship between SHMP dosage and Li₂O recovery and grade in the DDA system

The experimental investigation into the flotation behavior of single minerals revealed that sodium hexametaphosphate (SHMP) exhibits a pronounced inhibitory effect on quartz and a weaker inhibitory effect on lepidolite minerals, providing favorable conditions for effectively separating these two minerals. To achieve this, lepidolite was mixed with quartz in a 1:1 ratio, resulting in an ore with a Li_2O grade of 2.74%. As shown in Fig. 8, in the binary system of lepidolite and quartz, the concentrate obtained without SHMP closely resembles the original ore grade. This indicates that under weak acid conditions, DDA alone is insufficient to separate these two minerals. However, as the concentration of SHMP increases, numerous SHMP molecules are adsorbed onto the surface of quartz particles leading to continuous improvement in Li_2O grade within the concentrate while only slightly reducing recovery rate. At an SHMP dosage of 0.8×10^{-4} mol/L, the highest Li_2O grade achieved within the grade was 4.83%, with a recovery rate of 86.34%. These parameters represent optimal conditions for achieving effective separation between lepidolite and quartz through flotation processes. Therefore, the effective separation of lepidolite and quartz can be achieved by utilizing the appropriate dosage of sodium hexametaphosphate (SHMP), thereby addressing safety, environmental, and corrosion concerns associated with exclusive utilization of dodecylamine (DDA) flotation under strong acid conditions for this purpose.

3.2. Molecular dynamics simulation results

3.2.1. DDA adsorption on lepidolite and quartz surfaces

Through molecular dynamics simulation, the macroscopic phenomena can be elaborated from a microscopic point of view, and the forms of interactions and adsorption strengths between agents and mineral surfaces in aqueous environments can be observed and analyzed intuitively (Chen et al., 2023). This method is an important means to study the interaction between agents and minerals at the solid/liquid interface. In order to further analyze why DDA has stronger collecting properties for lepidolite than quartz under the same conditions, we chose the same agent concentration for MD simulation to study the adsorption process of DDA on the surfaces of lepidolite (001) and quartz (001), and in order to characterize the adsorption of DDA at the solid/liquid interface, we took the mineral surfaces as the origin of the coordinates, and calculated the N-atom in the head group of the DDA molecule density distribution as well as the adsorption energy, and these results are shown in Figs. 9 to 11, and Table 4.

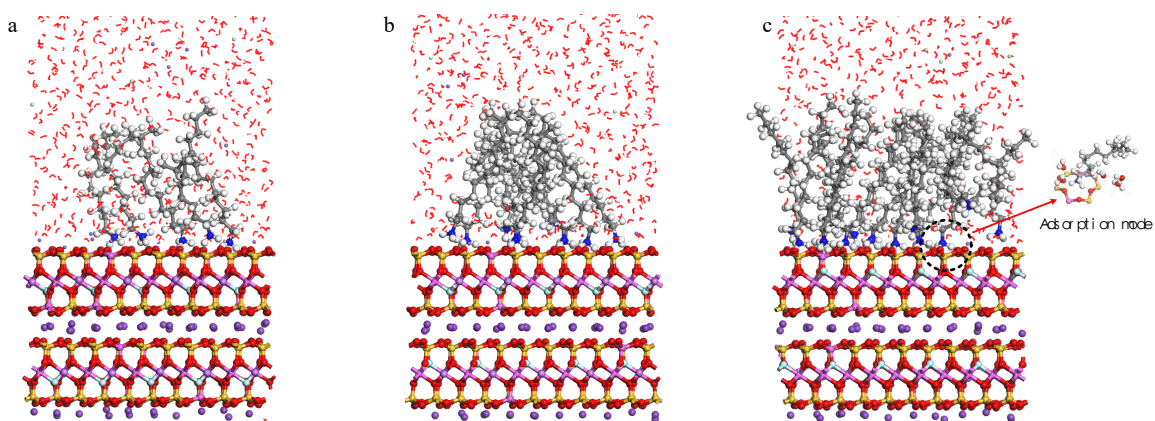


Fig. 9. Equilibrium configurations (a), (b), (c) after DDA adsorption at the solid/liquid interface on the surface of lepidolite (001) with 5, 10, and 15 DDA molecules, respectively

After the final molecular dynamics simulation, as illustrated in Fig. 9, the systems exhibit a relatively disordered state compared to their initial simulation state. In the aqueous environment, K^+ dissolution on the lepidolite surface results in surface electronegativity, leading to electrostatic attraction with the positively charged head group (amine group) in DDA. The hydrogen atom within the amine group forms a hydrogen bond with the oxygen atom located within the circular cavity of $[\text{Si}_{6-n}\text{Al}_n\text{O}_6]$ ($n=0, 1, 2$) on the lepidolite (001) surface, thereby enhancing adsorption and causing DDA to distribute like an "anchor" on this surface. Consequently, a monomolecular layer is formed at the solid/liquid interface.

Additionally, hydrogen bonds are established between oxygen atoms within circular cavities, further strengthening adsorption and promoting DDA distribution akin to an "anchor" on lepidolite's surface. Due to the amphiphilic nature of DDA, solidophilic groups adsorb onto mineral surfaces while hydrophobic carbon chains orient towards the water column. This type of adsorption can render minerals hydrophobic through collisional adhesion with air bubbles. At the DDA number of 10, an ordered arrangement of carbon chains is observed, resulting in aggregation and formation of a circular hydrophobic region. However, at higher concentrations (as shown in Fig. 9c), excessive DDA adsorption on lepidolite (001) leads to compensation for surface electrical differences caused by K^+ deficiency and unstable DDA adsorption tendencies with some desorption occurring; this does not imply decreased strength or saturation levels for DDA adsorption on lepidolite surfaces. Table 4 shows that the difference between the adsorption energies for 10/15 DDA systems on lepidolite surfaces was small (-147.70/-156.85 kcal/mol).

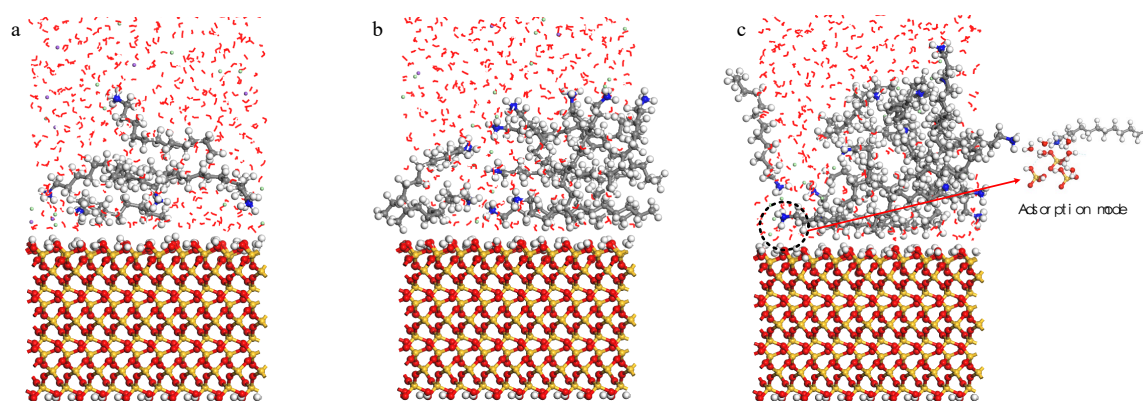


Fig. 10. Equilibrium configurations (a), (b), (c) after DDA adsorption at the solid/liquid interface on the quartz (001) surface with 5, 10, and 15 DDA molecules, respectively

Table 4. Adsorption energy of DDA on mineral surface

| Number of DDA | Lepidolite | | | Quartz | | |
|-------------------|------------|---------|---------|--------|--------|--------|
| | 5 | 10 | 15 | 5 | 10 | 15 |
| Energy (kcal/mol) | -131.13 | -147.70 | -156.85 | -58.40 | -56.22 | -61.31 |

Regarding the quartz surface, the adsorption behavior of DDA under aqueous conditions differs significantly from that on lepidolite surfaces. Fig. 10 depicts the equilibrium configurations of aqueous solutions containing 5, 10, and 15 DDAs after their adsorption onto the quartz surface respectively. It can be observed from Figs. 10a, 10b, and 10c that although DDA does adsorb onto the quartz surface, its interaction is distinct compared to its adsorption on lepidolite. Specifically, due to electrostatic repulsion between hydrogen atoms in hydroxyl groups present on the quartz surface and those in DDA's head group, direct interaction between them is hindered. Consequently, forming hydrogen bonds with oxygen atoms on the quartz surface becomes challenging for DDA. Instead, DDA primarily undergoes adsorption through hydrogen bonding facilitated by water molecules bonded to the quartz surface. This mode of adsorption results in lower stability compared to its counterpart on lepidolite surfaces and thus impedes effective DDA adsorption onto quartz surfaces. Furthermore, it is evident that different concentrations of DDA exhibit decreased values of adsorption energy when interacting with a quartz surface as opposed to a lepidolite one.

As shown in Fig. 11a, the adsorption of varying concentrations of DDA on the surface of lepidolite resulted in the formation of two distinct adsorption layers: a first layer primarily concentrated at 0.8 Å and a second layer occurring between 1.5 and 2.2 Å. These findings suggest a strong affinity between DDA and the surface of lepidolite. Additionally, as depicted in Fig. 11b, the distribution pattern of different DDA concentrations on quartz exhibited greater dispersion; when five DDAs were present, a minor characteristic peak appeared at 1.6 Å, although this peak was relatively small compared to a more prominent peak observed at 4 Å on quartz's surface although it is worth noting that this distance from

the quartz's surface has minimal impact. With increasing concentration levels, although DDA continued to adsorb onto the quartz's surface, concentration distribution analysis revealed peaks distributed within an interval ranging from 2 to 20 Å with varying degrees of intensity a clear indication that DDA exhibits lower adsorption strength on quartz's surface. In summary, these results demonstrate that DDA exhibits more stable adsorption behavior on lepidolite's surface compared to quartz rendering lepidolite more hydrophobic which aligns with flotation test outcomes, where using DDA as the sole collector leads to higher recovery rates for lepidolite than for quartz.

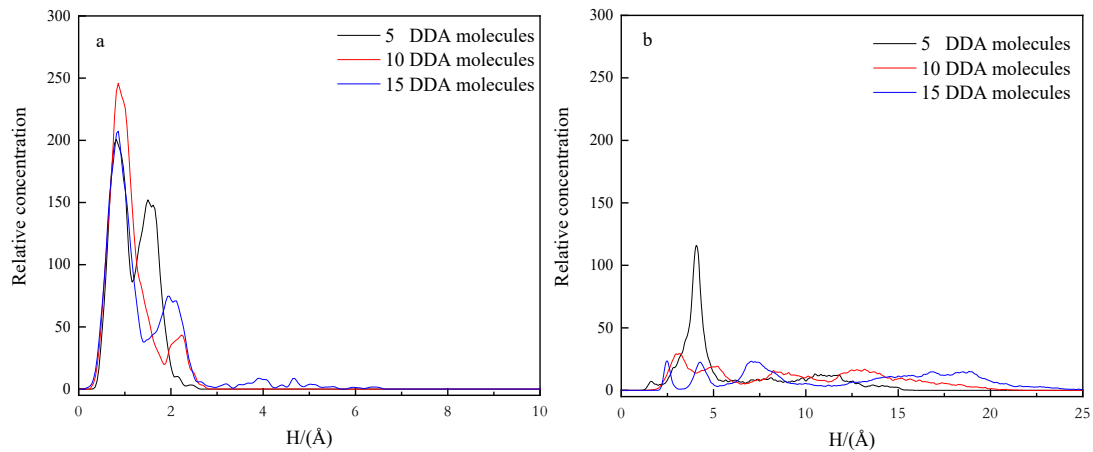


Fig. 11. Concentration distribution of different levels of DDA on the surface of two minerals (a) lepidolite (b) quartz

3.2.2. SHMP adsorption on lepidolite and quartz surfaces

To further investigate the enhanced inhibition of quartz by SHMP compared to lepidolite, we employed identical agent concentrations for MD simulation in order to analyze the adsorption process of SHMP on the (001) surfaces of both lepidolite and quartz. Moreover, to characterize the solid/liquid interface adsorption of SHMP, we computed both the density distribution of P atoms within the SHMP molecule and its corresponding adsorption energy. The obtained results are presented in Figs. 12-14 and Table 5.

After the final MD simulation, significant changes are observed in the aqueous solutions containing varying amounts of SHMP upon adsorption onto the surface of lepidolite, as depicted in Fig. 12. The lepidolite surface acquires a negative charge as a result of the deficiency of K^+ ions, as illustrated in Fig. 12a. Consequently, this electrostatic attraction selectively captures free Na^+ ions present in the aqueous solution and impedes the adsorption process of SHMP. Consequently, no adsorption of SHMP occurs

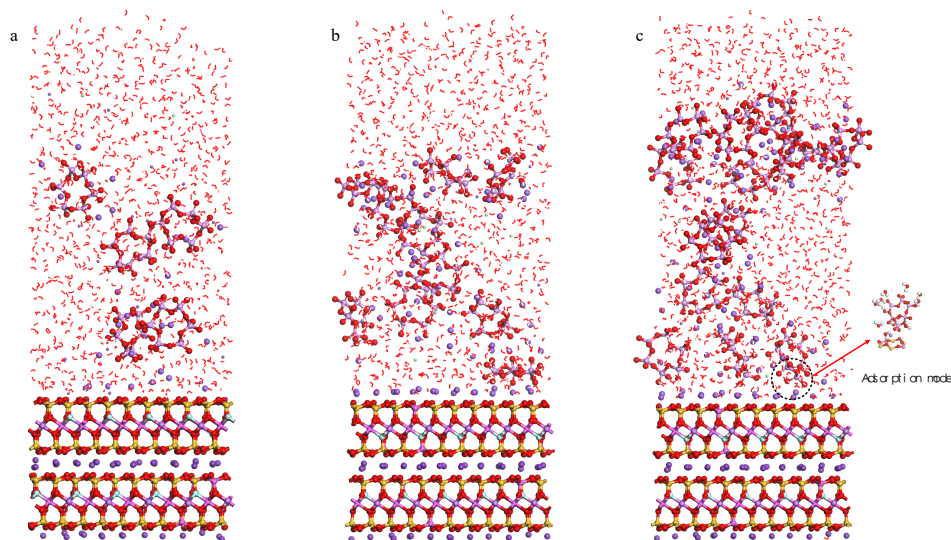


Fig. 12. Equilibrium configurations (a), (b), (c) after SHMP adsorption at the solid/liquid interface on the surface of lepidolite (001) with 5, 10, and 15 SHMP molecules, respectively (Na^+ is a light purple, and K^+ is a deep purple)

Table 5. Adsorption energy of SHMP on mineral surface

| Number of SHMP | Lepidolite | | | Quartz | | |
|-------------------|------------|--------|--------|---------|---------|---------|
| | 5 | 10 | 15 | 5 | 10 | 15 |
| Energy (kcal/mol) | 21.5 | -21.13 | -52.31 | -101.32 | -128.45 | -135.11 |

on the lepidolite surface. However, with increasing concentrations of SHMP (as shown in Fig. 12b), an increment in Na^+ concentration gradually compensates for potential deficiency at the lepidolite surface, resulting in weak electrostatic adsorption between a small amount of SHMP and lepidolite through Na^+ . Furthermore, when further increasing SHMP concentration (as demonstrated in Fig. 12c), a limited quantity of SHMP is absorbed via bound water molecules onto the lepidolite surface. It should be noted that this type of absorption is highly unstable, as evident from its relatively low adsorption energy (-52.31 kcal/mol) compared to DDA's adsorption energy on lepidolite's surface. These findings indicate that under aqueous conditions, as SHMP concentration increases, it does indeed get absorbed onto the surface of lepidolite; however, only a relatively small amount is actually adsorbed.

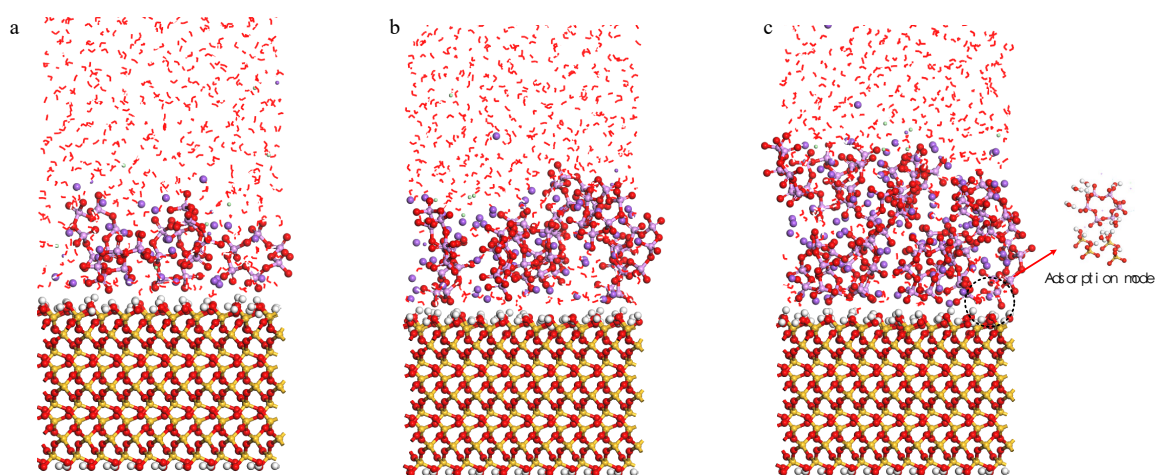


Fig. 13. Equilibrium configurations (a), (b), (c) after SHMP adsorption at the solid/liquid interface on the quartz (001) surface with 5, 10, and 15 SHMP molecules, respectively

The adsorption behavior of sodium hexametaphosphate (SHMP) on the quartz surface exhibited significant differences compared to that on the lepidolite surface under aqueous conditions, as illustrated in Fig. 13. Irrespective of the SHMP concentration, a robust adsorption phenomenon was observed on the quartz surface. This can be attributed to the formation of an adsorption layer with thicknesses ranging from 11 to 16 Å, wherein hydrogen bonding occurred between the oxygen atoms in SHMP and hydrogen atoms in hydroxyl groups present on the quartz surface. Furthermore, this interaction facilitated additional hydrogen bonding with water molecules, thereby enhancing both its adsorption capacity and hydrophilicity on the quartz surface. Notably, when compared to its adsorption onto lepidolite surfaces, SHMP exhibited lower adsorption energies onto quartz surfaces, indicating a stronger binding affinity towards quartz.

Based on Fig. 14a, it is evident that the distribution of SHMP on the surface of lepidolite in all three systems is relatively sparse, exhibiting varying degrees of dispersion ranging from approximately 5 to 40 Å away from the surface. Notably, two distinct peaks are observed at around 31 Å and 37 Å in the aqueous solution containing 10 and 15 SHMP molecules respectively; however, both peaks are significantly distant from the surface of lepidolite. This observation suggests a relatively low adsorption capacity of SHMP on the surface of lepidolite, with a majority being distributed within the aqueous solution itself. Furthermore, as depicted in Fig. 12b, there exists a disparity between the distribution pattern of SHMP on quartz surfaces compared to that on lepidolite surfaces. The initial characteristic peaks for all three systems appear closer to the quartz surface at distances approximately equal to 1.4 Å, 1.6 Å, and 1.7 Å respectively; indicating direct interaction between SHMP and quartz mineral surfaces. The remaining peaks exhibit a more concentrated distribution within an interval ranging from

about 1 to 15 Å distance from the surface suggesting high adsorption capability onto quartz surfaces where even just ten molecules can completely cover its entire area.

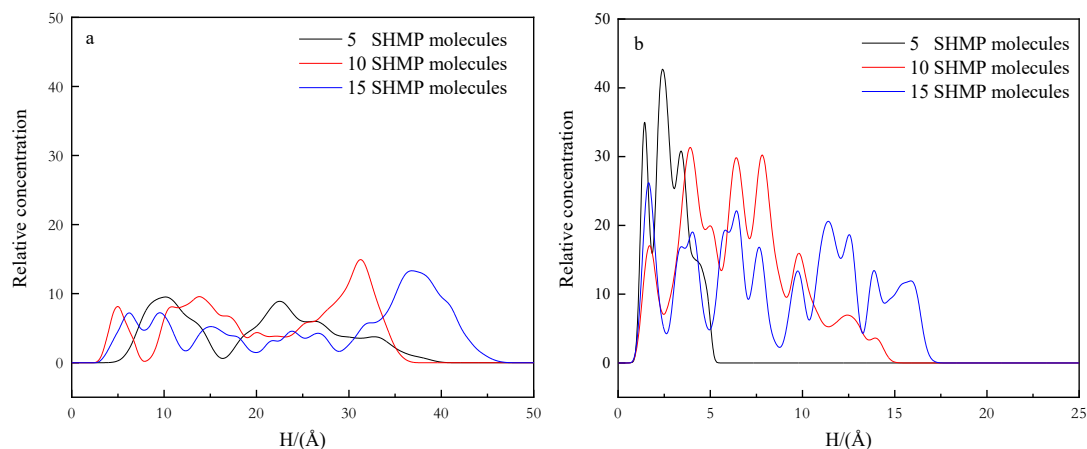


Fig. 14. Concentration distribution of different contents of SHMP on the surface of two minerals (a) lepidolite (b) quartz

3.2.3 SHMP and DDA co-adsorption on lepidolite and quartz surfaces

To enhance the comprehensibility of DDA adsorption on lepidolite and quartz surfaces after SHMP treatment, a simulation study was conducted to investigate DDA adsorption on the (001) surfaces of lepidolite and quartz in an aqueous environment following SHMP treatment, as illustrated in Fig. 15.

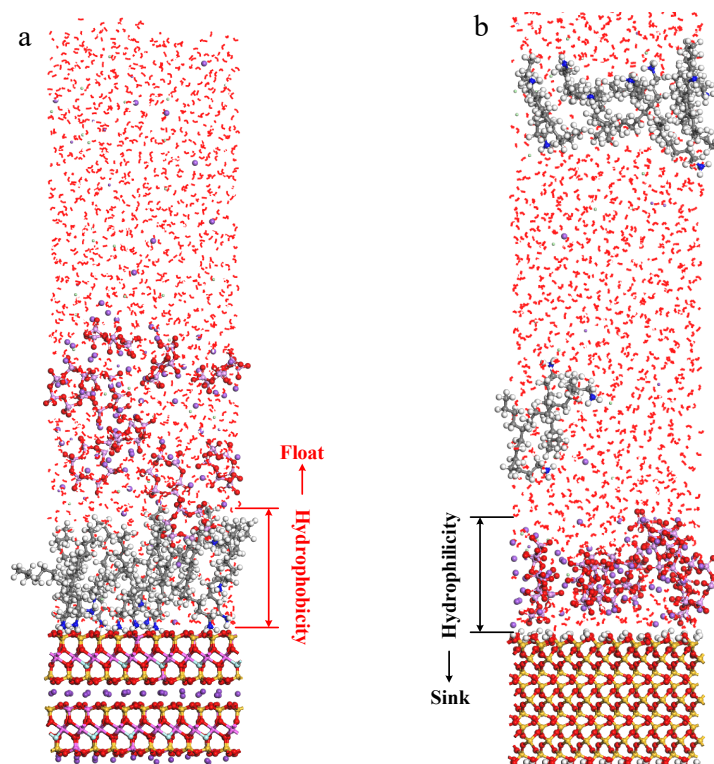


Fig. 15. Structure of 15 DDA adsorbed on lepidolite (001) and quartz (001) surfaces after being acted upon by 10 SHMP (Na^+ is a light purple, and K^+ is a deep purple)

According to the preceding text, the adsorption of SHMP on lepidolite is minimal. However, there are still available circular hole sites $[\text{Si}_{6-n}\text{Al}_n\text{O}_6]$ ($n=0,1,2$) for dodecylamine (DDA) adsorption on the surface of lepidolite after SHMP treatment. The final results from molecular dynamics simulations demonstrate that DDA can still effectively adsorb onto the surface of lepidolite even after being treated with SHMP. Due to its strong adsorption capability, the previously adsorbed SHMP can be desorbed.

This further confirms that the adsorption strength of DDA on the surface of lepidolite surpasses that of SHMP, which is advantageous for enhancing flotation recovery of lepidolite. On the contrary, since SHMP exhibits a robust affinity towards quartz surfaces, it completely covers and occupies these surfaces. Simultaneously, DDA has weaker adsorption compared to SHMP on quartz surfaces. As a result, DDA cannot displace or desorb already-adsorbed SHMP from quartz surfaces due to lack of suitable binding sites. Consequently, it fails to act upon or interact with quartz minerals during flotation processes and thus hampers their recovery in flotation operations.

3.3. Results of DDA adsorption on mineral surfaces after SHMP action

The MD simulation results reveal a significant disparity in the adsorption strength and quantity of sodium hexametaphosphate (SHMP) and dodecylamine (DDA) on lepidolite and quartz surfaces when they coexist. To investigate the influence of SHMP on DDA's adsorption ability on mineral surfaces, adsorption amount tests were conducted, with the corresponding results depicted in Fig. 16.

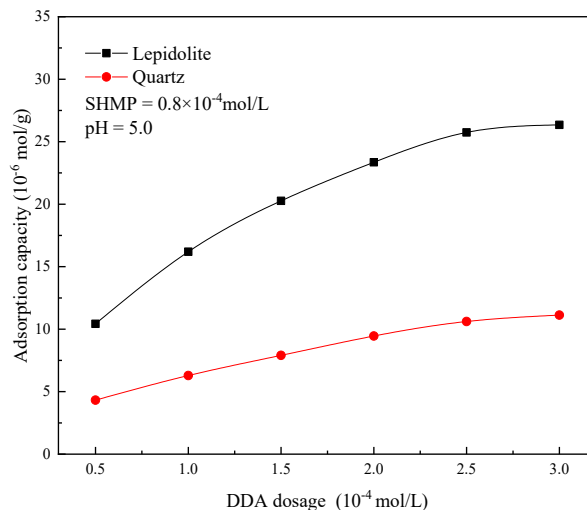


Fig. 16. DDA adsorption on mineral surface after SHMP action

The presence of SHMP in Fig. 16 demonstrates that with increasing amounts of dodecylamine (DDA), the adsorption of DDA on the lepidolite surface exhibits a rapid increase, while on the quartz surface it gradually reaches a plateau. Furthermore, within the measured range, the adsorption of DDA on the lepidolite surface consistently surpasses that on the quartz surface. These findings suggest that SHMP has a relatively minor impact on DDA's adsorption onto lepidolite; thus, significant quantities of DDA can still be absorbed by this surface, thereby enhancing flotation recovery rates for lepidolite. Conversely, SHMP strongly adheres to quartz surfaces resulting in minimal adsorption of DDA. This disparity in adsorption enables effective flotation separation. These results are consistent with molecular dynamics (MD) simulation outcomes.

3.5. Depression mechanism of SHMP

Upon dissolution in water, SHMP undergoes varying degrees of protonation, resulting in the hydroxylation of certain P atoms within the molecular chain to form the $-HPO_3^-$ unit. Additionally, different levels of polymerization of SHMP experience hydrolysis, leading to fragmentation of the chain molecules (Hu et al., 2003), as illustrated in Equation (3).



According to equation (3), it is evident that $[PO_3]$ serves as the primary component of sodium hexametaphosphate (SHMP) in an aqueous solution and plays a significant role in inhibiting quartz. The results from single mineral flotation experiments demonstrate that under strong acidic conditions, quartz exhibits extremely poor floatability when dodecylamine (DDA) is used as a trapping agent. This can be attributed to the facile hydroxylation of non-bridging oxygen atoms on the surface of quartz, resulting in electrostatic repulsion between hydrogen atoms in the hydroxyl group and hydrogen atoms

in DDA's headgroups. Consequently, achieving stable DDA adsorption on the surface of quartz becomes challenging, as confirmed by molecular dynamics (MD) simulation. As pH increases, the concentration of hydroxide ions (OH⁻) rises and combines with hydrogen atoms on the hydroxyl group of quartz surface, exposing oxygen atoms and rendering the surface negatively charged (as shown in Fig. 17). This allows positively charged DDA to interact with oxygen atoms, thereby enhancing quartz floatability. In other words, the degree of hydroxylation on the quartz surface plays a crucial role in separating lepidolite from quartz. Meanwhile, the added SHMP contains a valuable component [PO₃] that can adsorb onto the surface of quartz with lower hydroxylation degree under weak acid and neutral conditions through hydrogen bonding, where the O atoms in [PO₃] can be hydrophilic. Conversely, lepidolite's bridging oxygen atoms make it difficult for them to undergo hydroxylation while potassium ion solubilization within circular cavities on its surface [Si_{6-n}Al_nO₆] (n=0, 1, 2) leads to a negatively charged lepidolite surface which excludes SHMP adsorption. However, DDA's headgroup containing positive charges can firmly anchor onto these circular cavities' surfaces.

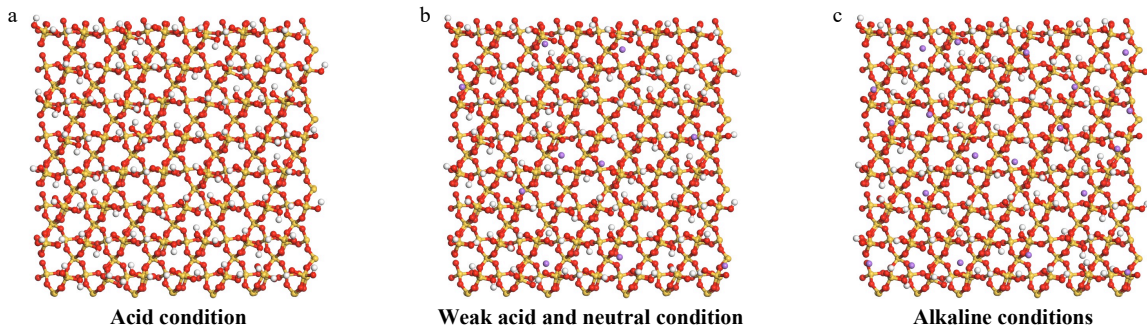


Fig. 17. Degree of hydroxylation on the surface of quartz (001) under different acid-base conditions (Na⁺ is used to label possible adsorption sites for DDA)

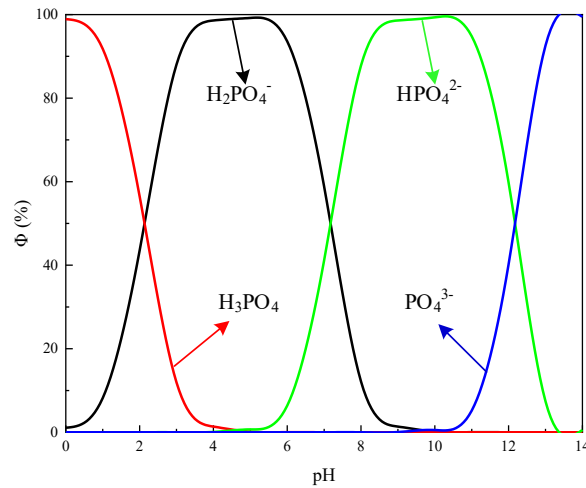


Fig. 18. Dominant components of SHMP hydrolysis under different pH

In addition to this, SHMP undergoes a small amount of hydrolysis, which is shown in equations (4 to 8).



The Φ -pH relationship for each hydrolyzed component of (NaPO₃)₆ can be depicted in Fig. 18 based on the aforementioned equilibrium. It is evident that H₃PO₄ dominates at pH < 2.0, H₂PO₄⁻ prevails

within the pH range of $2.0 < \text{pH} < 7.0$, HPO_4^{2-} becomes dominant at $7.0 < \text{pH} < 12.0$, and PO_4^{3-} takes over at $\text{pH} > 12.0$, indicating a transition towards PO_4^{3-} dominance beyond a pH value of 12.0. These findings imply that apart from the primary dissolution products with varying degrees of protonation, there are also minor hydrolysis components present in the SHMP solution; however, these dissociation and hydrolysis components exhibit limited selectivity and interact with mineral surfaces through electrostatic and hydrogen bonding interactions to influence their surface properties and flotation behaviors accordingly. This phenomenon is primarily manifested by a slight decrease in lepidolite recoveries observed after introducing SHMP into the system. Therefore, the action time of SHMP should not be too long to avoid too many hydrolysis products inhibiting lepidolite flotation. According to the aforementioned analysis, Fig. 19 illustrates the inhibitory mechanism of SHMP on quartz surfaces.

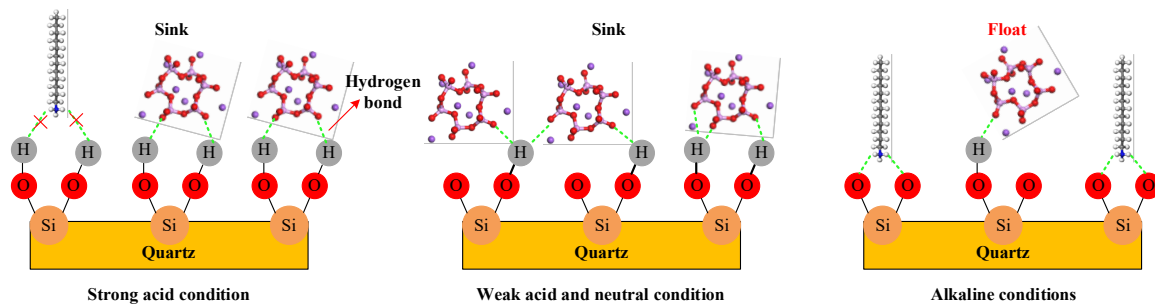


Fig. 19. Mechanism of quartz depression by SHMP

4. Conclusions

In this study, sodium hexametaphosphate (SHMP) was employed to achieve the flotation separation of lepidolite and quartz under weak acidic conditions. Molecular dynamics (MD) simulation revealed that the hydroxylation of non-bridge oxygen atoms on the surface of quartz influenced the adsorption behavior of dodecylamine (DDA), while it had no impact on SHMP adsorption. SHMP could indirectly enhance adsorption by forming hydrogen bonds with surface hydroxyl groups, thereby amplifying the hydroxylation of the quartz surface and preventing DDA adsorption, resulting in a more hydrophilic surface. On the other hand, due to K^+ dissolution in $[\text{Si}_{6-n}\text{Al}_n\text{O}_6]$ ($n=0,1,2$) rings on the lepidolite surface in an aqueous environment, it became negatively charged and attracted positively charged DDA molecules. The head group H atoms of DDA formed hydrogen bonds with O atoms on the lepidolite surface and further established a strong anchoring-like adsorption pattern within circular voids present in these ring structures. Moreover, all O atoms on the lepidolite surface were bridge O atoms; thus, no hydroxylation occurred making it difficult for SHMP to form hydrogen bonds and be absorbed onto this negatively charged lepidolite surface. Adsorption tests demonstrated that even after treatment with SHMP, significant amounts of DDA still adhered to lepidolite while only minimal DDA adsorbed onto quartz surfaces. In summary, in systems involving DDA as a collector, the degree of hydroxylation exhibited by quartz surfaces significantly impacts lepidolite resource recovery quality. Introducing SHMP can effectively enhance this degree under weak acid or neutral conditions which impedes DDA absorption leading to successful suppression of quartz impurities ultimately yielding high-quality lepidolite products.

Acknowledgements

This work was supported by the National Natural Science Foundation of China (No. 52274263); the Key Research and Development Project in Jiangxi Province (20214BBG74001).

References

- AI, G., YAN, H., WU, Y., LI, X., 2014. *Experimental Study on Mineral Processing of Comprehensive Recovery from a Ta-Nb Lepidolite Ore*. Non-metallic Mines, 37 (04): 4-6.
- BAI, Y., XU, M., WEN, W., ZHU, S., MO, W., YAN, P., 2023. *Synergistic mechanism of dodecylamine/octanol mixtures enhancing lepidolite flotation from the self-aggregation behaviors at the air/liquid interface*. Physicochemical Problems of Mineral Processin. 59(6), 176510.

- CHEN, J., CHU, X., CHENG, Y., SHU, Q., LING, Y., SHANG, H., MIN, F., 2023. *Application of molecular dynamics simulations in interface interaction of clay: Current status and perspectives*. *Asia-Pac J Chem Eng.* 18(5): e2955.
- CHOI, J., KIM, W., CHAE, W., 2012. *Electrostatically Controlled Enrichment of Lepidolite via Flotation*, *Materials Trans.*, 53, 12, 2191-2194.
- GUAN, Z., JIAO, F., WANG, X. QIN, W., FU, L., ZHANG, Z., LI, WEI., 2024. *New insights of inorganic phosphate inhibitors for flotation separation of calcium-bearing minerals*. *J. Cent. South Univ.* 31, 796–812.
- GUO, X., ZHANG, J., TIAN, Q., 2021. *Modeling the potential impact of future lithium recycling on lithium demand in China: A dynamic SFA approach*. *Renewable and Sustainable Energy Reviews.* 137, 110461.
- HEINZ, H., LIN, T., KISHORE M., EMAMI, F., 2013. *Thermodynamically consistent force fields for the assembly of inorganic, organic, and biological nanostructures: the interface force field*. *Langmuir.* 29, 1754-1765.
- HU, Y., CHEN X., WANG Y., 2003. *Selective action of phosphates on bauxite and kaolinite flotation*. *The Chinese Journal of Nonferrous Metals*, (01): 222-228.
- HUANG, Z., SHUAI, S., WANG, H., LIU, R., ZHANG, S., CHENG, C., HU, Y., YU, X., HE, G., FU, W., 2022. *Froth flotation separation of lepidolite ore using a new Gemini surfactant as the flotation collector*. *Separation and Purification Technology.* 282, 119122.
- HUANG, Z., LI, W., HE, G., SHEN, L., CHEN, X., SHUAI, S., LI, F., WANG, H., LIU, R., ZHANG, S., CHENG, C., OUYANG, L., YU, X., FU, W., 2022. *Adsorption Mechanism of Amidoxime Collector on the Flotation of Lepidolite: Experiment and DFT Calculation*. *Langmuir* 38 (50), 15858-15865.
- IRANNAJAD, M. EJTEMAEI, M. GHARABAGHI, M. 2009. *The effect of reagents on selective flotation of smithsonite-calcite-quartz*, *Minerals Engineering.* 22, 9-10, 766-771.
- KORBEL, C. FILIPPOVA, I.V. FILIPPOV, L.O. 2023. *Froth flotation of lithium micas – A review*. *Minerals Engineering.* 192, 107986.
- LIAO, R., WEN, S., LIU, JIAN., FENG, Q., 2022. *Flotation separation of fine smithsonite from calcite using sodium hexametaphosphate as the depressant in the Na₂S-Pb(II)-KIAX system*. *Separation and Purification Technology.* 295, 121245.
- LIU, K., 2023. *Research Progress in Flotation Collectors for Lepidolite Mineral: An Overview*. *Mineral Processing and Extractive Metallurgy Review.* 1-15.
- LIU, Z., JIAO, F., QIN, W., WEI, Q., 2022. *Collision-attachment law of lepidolite, feldspar and quartz with bubbles in the combined cationic and anionic collector system*. *Physicochemical Problems of Mineral Processing.* 58(6), 155324.
- LIU, C., MIN, F., LIU, L., CHEN, J. 2019. *Density Functional Theory Study of Water Molecule Adsorption on the α -Quartz (001) Surface with and without the Presence of Na⁺, Mg²⁺, and Ca²⁺*. *ACS Omega.*, 4(7), 12711-12718.
- LIU, J., PENG, B., ZHAO, L., BAI, F., LEI, Z., 2021. *Selection of an Appropriate Depressant in Flotation Separation of Molybdenum Oxide from Fluorapatite*. *Minerals.* 11, 1110.
- LIU, Z., SUN, Z., YU, J., 2015. *Investigation of dodecylammonium adsorption on mica, albite and quartz surfaces by QM/MM simulation*. *Molecular Physics.* 113(22), 3423-3430.
- LU, J., SUN, M., YUAN, Z., QI, S., TONG, Z., LI, L., MENG, Q., 2019. *Innovative insight for sodium hexametaphosphate interaction with serpentine*. *Colloids and Surfaces A: Physicochemical and Engineering Aspects.* 560, 35-41.
- MENG, Q., YUAN, Z., XU, Y., DU, Y., 2019. *The effect of sodium silicate depressant on the flotation separation of fine wolframite from quartz*. *Separation Science and Technology*, 54(8), 1400-1410.
- PENG, W., ZHANG, L., QIU, Y., SONG, S., 2016. *Depression effect of corn starch on muscovite mica at different pH values*. *Physicochemical Problems of Mineral Processing.* 52(2), 780-788.
- TADESSE, B., MAKUEI, F., ALBIJANIC, B., DYER, L., 2019. *The beneficiation of lithium minerals from hard rock ores: A review*. *Minerals Engineering.* 131, 170-184.
- TIAN, M., GAO, Z., JI, B., FAN, R., LIU, R., CHEN, P., SUN, W., HU, Y., 2018. *Selective Flotation of Cassiterite from Calcite with Salicylhydroxamic Acid Collector and Carboxymethyl Cellulose Depressant*. *Minerals.* 8, 316.
- WANG, J.; GAO, Z.; GAO, Y.; HU, Y.; SUN, W. 2016. *Flotation separation of scheelite from calcite using mixed cationic/anionic collectors*. *Miner. Eng.* 98, 261-263.
- WANG, L., SHEN, L., SUN, W., ZHANG, X., ZHANG, Y., WANG, Y., 2022. *Selective flotation separation of smithsonite from dolomite by using sodium hexametaphosphate as a depressant*. *Colloids and Surfaces A: Physicochemical and Engineering Aspects.* 651, 129621.
- WANG, L., SUN, W. LIU, R., 2014. *Mechanism of separating muscovite and quartz by flotation*. *Cent. South Univ.* 21, 3596-3602.

- WEI, Q., FENG, L., DONG, L., JIAO, F., QIN, W., 2021. *Selective co-adsorption mechanism of a new mixed collector on the flotation separation of lepidolite from quartz*. *Colloids and Surfaces A: Physicochemical and Engineering Aspects*. 612, 125973.
- VIECELI, N., DURÃO, F. O. GUIMARÃES, C., NOGUEIRA, C. A. PEREIRA, M. F.C. MARGARIDO, F., 2016. *Grade-recovery modelling and optimization of the froth flotation process of a lepidolite ore*. *International Journal of Mineral Processing*. 157, 184-194.
- XIAO, C., WANG, BIN., ZHAO, D., WANG C., 2023. *Comprehensive investigation on Lithium batteries for electric and hybrid-electric unmanned aerial vehicle applications*. *Thermal Science and Engineering Progress*. 38, 101677.
- YANG, Z., LI, M., LIN, Y., YAO, W., WU, Y., CUI, R., 2023. *Floatability of Fluorite and Calcite Inhibited by Sodium Hexametaphosphate via Ultrasonic Activation*. *Minerals*. 13, 1504.
- ZHANG, H., LIN, S., GUO, Z., SUN, W., ZHANG, C., 2023. *Selective separation mechanism of hematite from quartz by anionic reverse flotation: Implications from surface hydroxylation*. *Applied Surface Science*. 614, 156056.
- ZHANG, Z., WEI, Q., JIAO, F., QIN, W., 2023. *Role of nanobubbles on the fine lepidolite flotation with mixed cationic/anionic collector*. *Powder Technology*. 427, 118785.
- ZHANG, H., ZHOU, F., YU, H., LIU, M., 2021. *Double roles of sodium hexametaphosphate in the flotation of dolomite from apatite*. *Colloids and Surfaces A: Physicochemical and Engineering Aspects*. 626. 127080.